doi:10.26443/seismica.v5i1.2144

SEISMICA

Temporal changes in surface afterslip along the 2016 Kumamoto earthquake rupture revealed by repeated field surveys

Yoshiya Iwasa *[1], **Yasuhiro Kumahara** [2], **Yuya Sumitani**[3], **Yuichiro Tabuchi**[3]

[1]Faculty of Education, University of Teacher Education Fukuoka, 1-1, Akamabunkyo-machi, Munakata, Fukuoka 811-4192, Japan, [2]Graduate School of Humanities and Social Sciences, Hiroshima University, 1-1-1, Kagamiyama, Higashi-Hiroshima, Hiroshima 739-8524, Japan, [3]Formerly at Graduate School of Humanities and Social Sciences, Hiroshima University, 1-1-1, Kagamiyama, Higashi-Hiroshima, Hiroshima 739-8524, Japan

Author contributions: *Conceptualization*: Y. Kumahara. *Data Curation*: Y. Iwasa, Y. Sumitani. *Formal Analysis*: Y. Iwasa, Y. Sumitani. *Funding Acquisition*: Y. Iwasa, Y. Kumahara, Y. Sumitani. *Investigation*: Y. Iwasa, Y. Kumahara, Y. Sumitani, Y. Tabuchi. *Methodology*: Y. Kumahara. *Project Administration*: Y. Kumahara. *Resources*: Y. Kumahara. *Supervision*: Y. Kumahara. *Visualization*: Y. Iwasa. *Writing – original draft*: Y. Iwasa. *Writing – review & editing*: Y. Kumahara, Y. Sumitani, Y. Tabuchi.

Abstract Surface afterslip can persist over several years, with displacements reaching tens of centimeters. Such deformations can damage structures, making it crucial to understand their temporal changes for effective post-earthquake reconstruction. Following the 2016 Kumamoto earthquake sequence, surface afterslip was observed at seven sites along a 5.7 km section of the fault. This segment is the junction between two adjacent active faults, where surface ruptures occurred during both the foreshock and the mainshock. Based on repeated field measurements, the surface afterslip persisted for 6–7 years following the mainshock. The cumulative displacement amounted to 10–40 cm. Compared with previous studies, its persistence is relatively long, whereas the displacement is comparable to reported values. The postseismic and coseismic displacements were nearly identical at the southern site of the fault, suggesting that distinguishing between coseismic and postseismic displacements in paleoseismic trenching or geomorphic offset studies can be challenging. Surface afterslip, which can persist for several years, may cause further damage to surface and subsurface infrastructure that has been repaired or restored following earthquakes. When planning post-earthquake restoration, it is necessary to determine whether surface afterslip is occurring and to estimate when it will cease.

要旨 2016年熊本地震の発生後、断層沿いの5.7 kmの区間において地表余効すべりが生じた。現地において計測を繰り返した結果、地表余効すべりは6〜7年間継続しており、累積変位量は場所によって10〜40 cmであった。過去の研究と比較すると、地表余効すべりの継続期間は比較的長く、変位量は同程度であった。南部の地点では地表余効すべりと本震の変位量が同程度であり、トレンチ掘削調査や地形に基づく変位量調査において両者を区別することが困難な場合があることが示唆される。地表余効すべりは、地震後に修復されたインフラにさらなる損傷をもたらす可能性がある。地震からの復旧では、地表余効すべりの発生の確認や、その終息時期の推定が重要であると考えられる。

Non-technical summary Following the 2016 Kumamoto earthquake sequence, surface displacements due to surface afterslip were observed at seven sites along a 5.7 km section of the fault. Surface afterslip caused cracks on the road, displacement of painted road markings, and displacement of concrete block walls. Repeated field measurements showed that the surface afterslip persisted for 6–7 years. The total displacement amounted to 10–40 cm. Surface afterslip, which can last for several years, may cause further damage to surface and subsurface infrastructure that has been repaired after earthquakes. When planning post-earthquake restoration, it is important to check whether surface afterslip is occurring and to estimate when it will cease.

Production Editor:
Andrea Llenos
Handling Editor:
Wenbin Xu
Copy & Layout Editor:
Hannah F. Mark

Signed reviewer(s):
Shinji Toda

Received:
December 3, 2025
Accepted:
March 17, 2026
Published:
April 6, 2026

1 Introduction

Intraplate active faults often generate surface ruptures that clearly delineate the fault movement at the ground surface. Such coseismic surface displacements provide key evidence for understanding the mechanical behavior of the upper crust and for constraining fault geometry and slip distribution (Wesnousky, 2008; Nurminen et al., 2022). However, the surface deformation does not necessarily end at the time of rupture.

Postseismic deformation occurs following large interplate and intraplate earthquakes and has been detected by satellites and GNSS networks over a wide area around the source fault (Ozawa et al., 2012; Hong and Liu, 2021; Dhar et al., 2023; Shu et al., 2024; Suito, 2025;

*Corresponding author: iwasa-y@fukuoka-edu.ac.jp

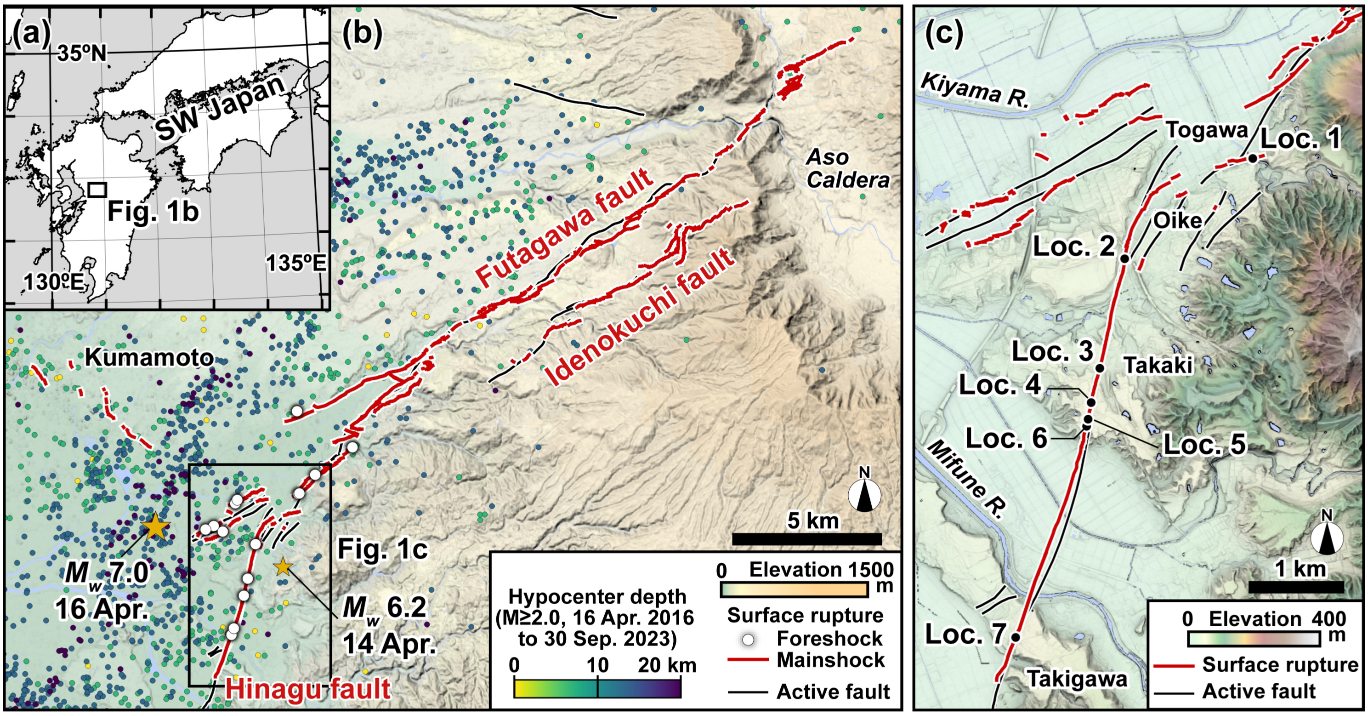

Figure 1 (a) Index map of the study area. (b) Distribution of the epicenters and surface ruptures associated with the Kumamoto earthquake sequence. Yellow stars indicate the epicenters of the largest foreshock and the mainshock, and the dots indicate the aftershocks following the mainshock. (c) Enlarged map of the study area. Black circles indicate locations where the surface afterslip was observed. Red lines and white circles in Figure 1b and c indicate the surface ruptures associated with the foreshock and the mainshock, respectively (Kumahara et al., 2022). Black lines in Figure 1b and c indicate the active fault (Nakata and Imaizumi, 2002).

Noda et al., 2017). Mechanisms driving postseismic deformation include viscoelastic relaxation in the lower crust and upper mantle, poroelastic deformation involving upper-crust fluids, and afterslip along the rupture zone (Hong and Liu, 2021; Churchill et al., 2022; Noda et al., 2017). While afterslip has been detected in recent years by satellites and GNSS networks, it has sometimes been observed as surface deformation along fault traces (hereafter referred to as surface afterslip). The surface afterslip can persist over several years, with displacements reaching tens of centimeters (Scholz et al., 1969; Lienkaemper and McFarland, 2017; Cakir et al., 2005). These deformations could cause structures that were damaged by an earthquake and subsequently repaired to be damaged again. Therefore, understanding the temporal changes of surface afterslip is crucial for effective post-earthquake reconstruction. Although numerous surface-rupturing earthquakes have occurred in Japan, there are few cases of surface afterslip that have been observed, except for the 2016 Kumamoto earthquake sequence (Shirahama et al., 2016; Toda et al., 2021). In particular, few cases worldwide where quantitative displacement has been directly and continuously captured at the ground surface.

The Kumamoto earthquake sequence, consisting of a M_w 6.2 foreshock and a M_w 7.0 mainshock, occurred on 14 April and 16 April 2016, respectively, in central Kyushu, southwest Japan. In the foreshock, 6-km-long surface ruptures occurred mainly along the northern Hinagu fault near its structural junction with the adjacent Futagawa fault (Sugito et al., 2016, Figure 1). The maximum dextral displacement of the surface rupture was 50 cm (Sugito et al., 2016). During the mainshock, ~30-km-long dextral slip-dominated surface ruptures with a maximum displacement of 2.3 m occurred along the northern Hinagu fault, the entire Futagawa fault, and the Idenokuchi fault (Fujiwara et al., 2016; Shirahama et al., 2016; Toda et al., 2016; Kumahara et al., 2022, Figure 1). Postseismic deformation was detected by satellite over a wide area after the Kumamoto earthquake (Fujiwara et al., 2016; Shirahama et al., 2016; Pollitz et al., 2017; Hashimoto, 2020; Himematsu and Furuya, 2020; Milliner et al., 2020; Liu et al., 2024). Fujiwara et al. (2016) and Pollitz et al. (2017) indicated that afterslip occurred on the northern part of the Hinagu fault within the first year following the Kumamoto earthquake. Liu et al. (2024) indicated that, during the five years following the Kumamoto earthquake, postseismic deformation occurred at shallow depths on the northern part of the Hinagu fault. Correspondingly, surface afterslip was observed. In the northern part of the Hinagu fault, Shirahama et al. (2016) reported that the surface rupture displacement increased by 10 cm within 12 days after the earthquake. In a 2 km section of the northern part of the Hinagu fault, Toda et al. (2021) reported that ~20 cm of displacement occurred within one year after the earthquake, and that a few centimeters of displacement occurred during three years from 2017 to 2020 at another site. However, the temporal changes in displacement over longer timescales (≥5 years) are unknown. Considering its structural junction with the Futagawa fault and its history of recurring surface deformation (foreshock, mainshock, and postseismic phases), the northern part of the Hinagu fault likely hosts a complex subsurface architecture. Therefore, elucidating the temporal change in surface afterslip within this segment can yield critical insights into physical mechanisms, such as the effects of stress changes at fault junctions and the spatial variability in frictional properties at shallow depths.

In this study, we present the characteristics of temporal changes in surface afterslip following the Kumamoto earthquake sequence based on field measurements.

2 Methods

To reveal the temporal change in surface afterslip, we conducted six field surveys between March 2020 and September 2023. First, we conducted field surveys to determine whether surface afterslip had occurred along the surface ruptures along the Futagawa and the Hinagu faults associated with the Kumamoto earthquake. In the field, we used linear features such as road lines and concrete block walls as markers of surface afterslip. We focused on three sites (Locs. 2, 6, and 7) where clear dextral displacements were observed and recorded their temporal changes by measuring the linear features with a total station (Nikon NST-200CN). Because we could not install permanent benchmarks, measuring identical coordinates across survey epochs was impractical. Instead, we maintained measurement consistency by tracing identical linear features, such as repeatedly surveying a specific edge of a white road line during each campaign (Figure S1). To calculate offsets, we first defined the fault strike as the general strike of the surface ruptures identified at each site. We projected all displacement values parallel to this strike. Next, guided by field observations and plotted survey data, we defined undeformed reference sections on opposite sides of the primary deformation zone using straight segments of these linear features. For each survey epoch, we calculated the mean position of the points within each reference section and determined the fault displacement as the difference between these two positions. We estimated the associated measurement uncertainty (represented by error bars in Figure 4) by calculating the root sum square of the standard errors of the mean for both reference sections. However, as described later, these reference markers reflected displacements that occurred after repairs conducted in the first half of 2017. Consequently, the displacements during the first year after the mainshock remain unknown. To capture the early displacement after the mainshock, we measured structures that preserved the coseismic displacement from the mainshock.

3 Results

Investigation of all surface ruptures revealed surface afterslips, including cracks with dextral displacement, at seven sites along a 5.7 km section of the northern Hinagu fault (Figure 1). Unlike surface ruptures, surface afterslip was discontinuous and occurred only locally at each site. This may be due not only to surface structural variations and the availability of clear reference markers but also to subsurface geological heterogeneity (Toda et al., 2021). Here, we describe the characteristics of the surface afterslip. The locations and photographs are shown in Figures 1 and 2, respectively. Site coordinates, measurement timing, and displacement values are provided in the associated dataset (see Data and code availability).

At Loc. 1 in Togawa, we found N80°E-trending cracks on the road on 28 March 2020 (Figure 2a, b). The crack has a north-side-down step of ~1 cm. At this site, a 30 cm north-side-down surface rupture occurred during the mainshock of the Kumamoto earthquake sequence (Kumahara et al., 2022), and the road was subsequently repaired on 30 November 2017. Therefore, the cracks observed on 28 March 2020 likely formed during the two and a half years following the repair. Although no increase in vertical displacement was detected, the cracks appeared to have lengthened by 18 December 2022 compared with 28 March 2020 (Figures 2a, b).

At Loc. 2 in Oike, we found N10°E-trending cracks with a left-stepping *en-echelon* structure on the road on 29 March 2020 (Figure S1). The white line and pavement joint were displaced dextrally (Figure 2c). Toda et al. (2021) also observed these cracks and dextral displacements in July 2020. At this site, a few-centimeter dextral surface rupture was observed after the foreshock, and a 55 cm dextral surface rupture occurred during the mainshock of the Kumamoto earthquake sequence (Kumahara et al., 2022). The road was subsequently repaired on 28 April 2017. Therefore, the dextral displacement of the road line at Loc. 2 has recorded cumulative displacement since April 2017. We measured the road line shown in Fig. 2c four times with a total station during the period from 2020 to 2022. From March 2020 to August 2022, the dextral displacement of the road line increased from 5.9 cm to 8.8 cm (Figure 3a). Based on the road repair date (28 April 2017) and the measured displacement in August 2022 (8.8 cm), we estimated the slip rate of surface afterslip from April 2017 to August 2022 as 1.7 cm/year. Note that the pavement was repaired again between August and December 2022, precluding determination of surface afterslip. Furthermore, 15 m south of the road line, a ditch recorded the displacement associated with both the mainshock and the surface afterslip (Figure S3a). The ditch was displaced dextrally by 69.9 cm in September 2023. Although the measurement methods differed, considering that a 55 cm dextral displacement occurred during the mainshock, the cumulative surface afterslip after the mainshock was 14.9 cm. At Loc. 3 in Takaki, we found N15°E-trending cracks and a small graben-like depression on the road on 29 March 2020 (Figures 2d, e). The small graben-like depression was first observed on 29 March 2020 and was repaired and leveled by 27 September 2020 (Figure 2d). It reappeared on 4 September 2021 with a depth of 3.0 cm and deepened to 4.5 cm by 10 August 2022 (Figures 2e, S2). The pavement joint was displaced dextrally by 3.5 cm (Figure 2f). Toda et al. (2021) also reported these cracks and dextral displacements of approximately 3 cm in August 2020. At

Figure 2 Photographs of the surface afterslip along the Hinagu fault. The locations are shown in Figure 1. Red arrows indicate the location of surface afterslips.

this site, cracks had been observed after the foreshock, and a 30 cm dextral surface rupture occurred during the mainshock (Kumahara et al., 2022). The road had been repaired in April 2017; thus, the cracks observed on 29 March 2020 likely formed during the three years following the repair.

At Loc. 4 in Takaki, we found N18°E-trending cracks with a left-stepping *en-echelon* structure on the road on 29 March 2020 (Figure 2g). The pavement joint was displaced dextrally by 5.8 cm. Toda et al. (2021) had observed this *en-echelon* structure on 5 April 2017, reporting that it had grown to connect the open cracks formed as surface ruptures during the mainshock. A comparison of photographs from 5 April 2017, taken by Toda et al. (2021), and 29 March 2020 indicates that the road had been repaired, suggesting that surface afterslip was still ongoing in 2020.

At Loc. 5 in Takaki, we found N14°E-trending cracks with a left-stepping *en-echelon* structure on the parking lot on 11 August 2022 (Figure 2h). The pavement joint was displaced dextrally by 2 cm (Figure 2i). Based on information from residents, a 40 cm of dextral surface rupture had been observed after the mainshock at this site. The parking lot was paved in July 2021, indicating that the cracks likely formed within one year following the paving.

At Loc. 6 in Takaki, we found the concrete block wall was displaced dextrally on 28 March 2020 (Figure 2j). Toda et al. (2021) also reported this displacement in 2018. At this site, a 50 cm dextral surface rupture occurred during the mainshock of the Kumamoto earthquake sequence (Kumahara et al., 2022), and the wall was subsequently repaired in February 2017. Therefore, the displacement observed on 28 March 2020 likely formed during the three years following the repair. We measured the concrete block wall shown in Figure 2j six

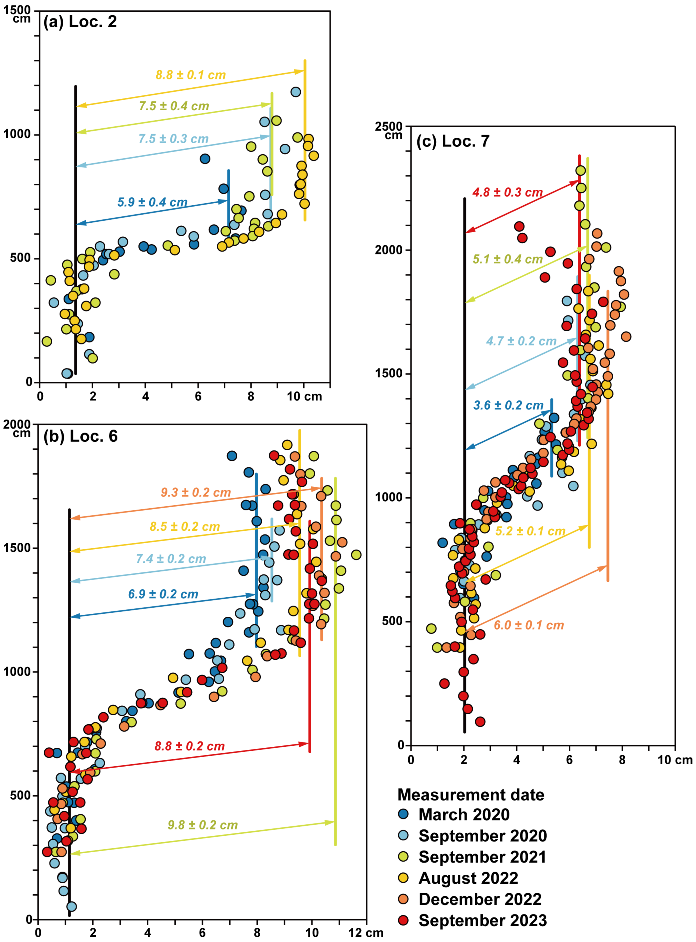

Figure 3 Results of repeated measurements of the linear objects at Locs. 2, 6, and 7. Locations are shown in Figure 1. Dots indicate measurement points using a total station colored by measurement date. Lines represent reference marker using the average value of the undeformed section.

times with a total station. From March 2020 to September 2023, the dextral displacement of the concrete block wall increased from 6.9 cm to ~8 cm (Figure 3b). The value for September 2021 deviates considerably from the trend observed in the other periods, suggesting that it represents an outlier likely caused by measurement error. Based on the road repair date (February 2017) and the measured displacement in September 2023 (8.8 cm), we estimated the slip rate of surface afterslip from February 2017 to September 2023 as 1.3 cm/year. Furthermore, 140 m north of the concrete block wall, another concrete block wall recorded the displacement associated with both the mainshock and the surface afterslip (Figure S3b). Toda et al. (2021) reported that this concrete block wall had displaced dextrally by 20 cm within one year of the main shock. We measured the displacement of this concrete block wall to be 91.8 cm in September 2023. Although the measurement methods differed, considering that a 50 cm dextral displacement occurred during the mainshock, the cumulative surface afterslip after the mainshock was 41.8 cm. The apparent discrepancy between this 41.8 cm value and the ~8.8 cm displacement observed at Loc. 6 (140 m away) can be attributed to several factors. Beyond potential spatial variations in the displacement along the fault, we must also consider the possibility that the apparent displacement was partially influenced by localized deformation or tilting of the concrete structure itself, rather than being purely tectonic. Additionally, differences in the observation windows likely contributed to this discrepancy. Specifically, because the wall at Loc. 6 was repaired in February 2017, it failed to capture the surface afterslip that occurred during the first year following the mainshock. As Toda et al. (2021) indicated, surface afterslip is larger immediately following the earthquake. Furthermore, differences in measurement methods—such as the use of a tape measure in Toda et al. (2021) versus the total station used in this study—may have also influenced the results.

At Loc. 7 in Takigawa, we found that the white line on the road was displaced dextrally on 28 March 2020 (Figure 2k). At this site, an 11 cm of dextral surface rupture occurred during the mainshock (Kumahara et al., 2022), and the road was subsequently repaired in April 2017. Therefore, the displacement observed on 28 March 2020 likely formed during the three years following the repair. We measured the displacement of the road line shown in Fig. 2k six times with a total station. From March 2020 to September 2023, the dextral displacement of the road line increased from 3.6 cm to ~5 cm (Figure 3c). The value for December 2022 deviates considerably from the trend observed in the other periods,

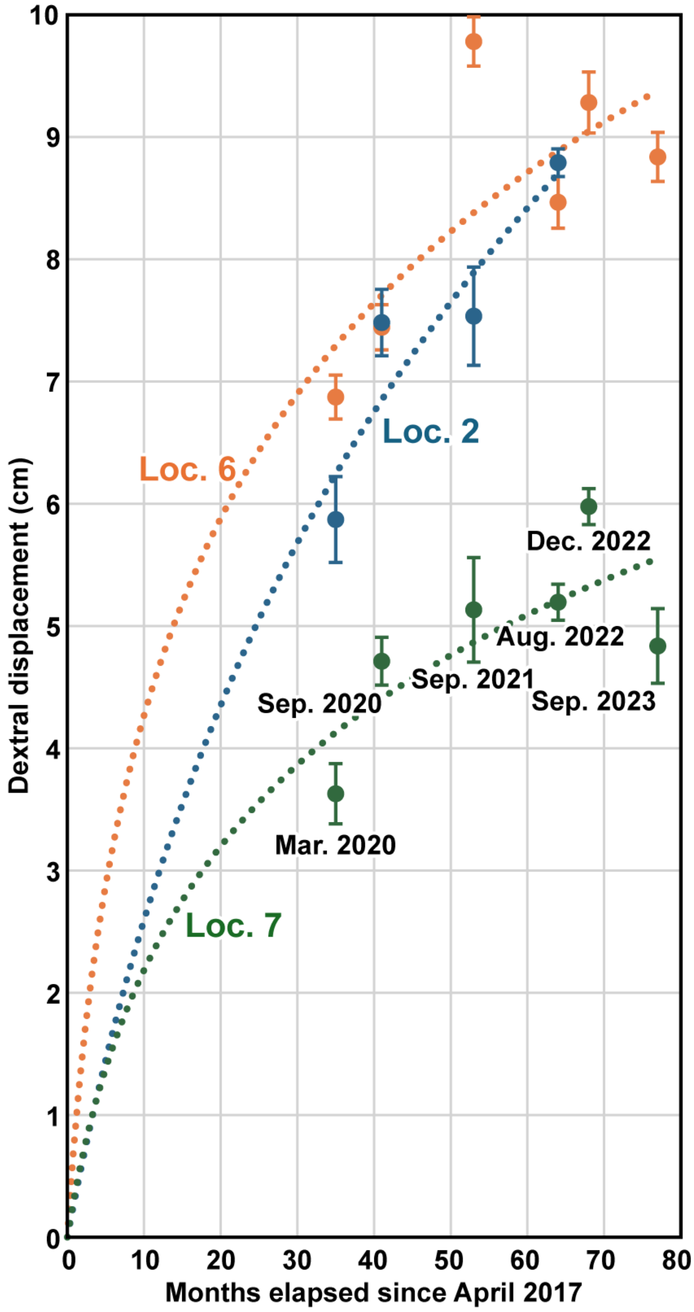

Figure 4 Temporal changes in dextral displacement since April 2017 at Locs. 2, 6, and 7. Locations are shown in Figure 1.

suggesting that it represents an outlier likely caused by measurement error. Based on the road repair date (April 2017) and the displacement measured in September 2023 (4.8 cm), we estimated the slip rate of surface afterslip from April 2017 to September 2023 as 0.7 cm/year. Furthermore, immediately south of the road line, a ditch recorded the displacement associated with both the mainshock and the surface afterslip (Figure S3c). The ditch was displaced dextrally by 21.2 cm in September 2023. Although the measurement methods differed, considering that an 11 cm dextral displacement occurred during the mainshock, the cumulative surface afterslip after the mainshock was 10.2 cm.

In the northern part of the Hinagu fault, surface afterslip continued after 2020. As afterslip typically follows a decaying trend (Nakao et al., 2019), we fitted the temporal changes of the cumulative displacement in Figure 4 using a logarithmic function. Repeated measurements and fitted curves indicate that the amount of displacement continued to increase through September 2023 (Figure 4), although the rate of increase has gradually been declining. Furthermore, during our latest field survey in February 2025, we detected no newly discernible surface displacement. This observation, combined with the logarithmic decay curves, suggests that the surface afterslip has decayed and has nearly terminated.

4 Discussion and conclusion

In this study, we present the temporal changes in surface afterslip following the Kumamoto earthquake. The

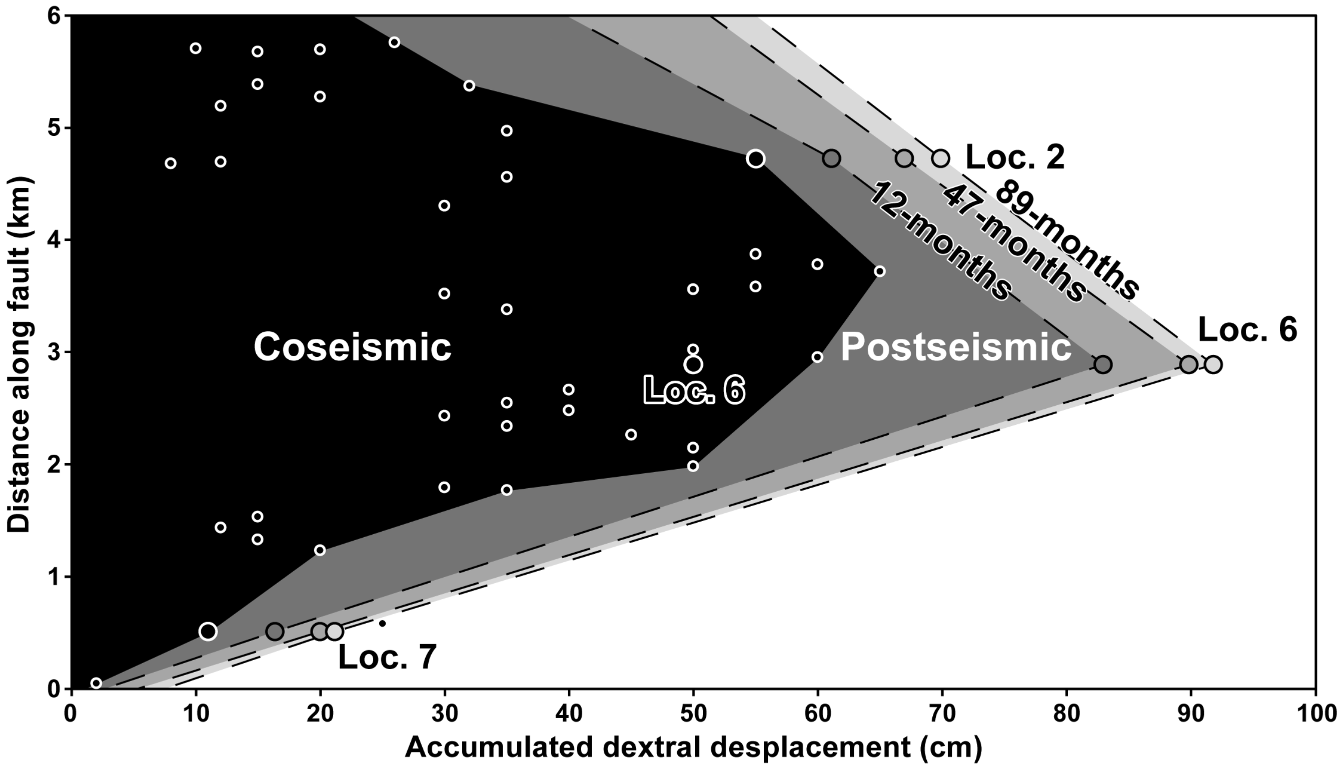

Figure 5 Accumulated displacement at Locs. 2, 6, and 7 plotted against distance along the fault 12, 47, and 89 months after the mainshock (Bigger dots). The coseismic displacement indicated by black dots is based on Kumahara et al. (2022).

cumulative displacement of the surface afterslip following the mainshock amounted to 10–40 cm. Although the results were limited to three sites, when we compared the postseismic/coseismic displacement ratio at each site, we found that the northern site (Loc. 2), where coseismic displacement was large, exhibited a small postseismic/coseismic ratio of 27% (Figure 5). In contrast, the southern sites (Locs. 6 and 7), where coseismic displacement was small, exhibited a large postseismic/coseismic ratio greater than 80% (Figure 5). At these southern sites, surface afterslip nearly equaled the coseismic displacement; this elevated proportion likely compensates for insufficient coseismic stress release during the mainshock (Toda et al., 2021; Shu et al., 2024; Suito, 2025). At the southern sites where coseismic displacement was small, the proportion of surface afterslip may have been large because coseismic stress release was insufficient (Toda et al., 2021; Shu et al., 2024; Suito, 2025). If such phenomena also occurred in the past, we would have difficulty distinguishing coseismic from postseismic displacement in paleoseismic trenching or geomorphic offset studies. This could lead to overestimation of past coseismic displacement and earthquake magnitude derived from trench or geomorphic evidence, and therefore requires careful interpretation (Baize and Scotti, 2015).

We found that surface afterslip persisted for 6–7 years following the Kumamoto earthquake along a 5.7 km section of the northern Hinagu fault. We estimated the average slip rate for the period from 2017 to 2023 to be 0.7–1.7 cm/year. From a geodetic perspective, Hashimoto (2020) reported that westward horizontal displacement on the eastern side of the northern end of the Hinagu fault could have reached 6 cm by the winter of 2016. Hashimoto (2020) estimated this westward slip rate as 6 cm/year by April 2018 (two years after the earthquake). Liu et al. (2024), based on GPS observations, showed that postseismic deformation persisted with displacements of a few centimeters for four to five years after the earthquake. Furthermore, Nakao et al. (2019) demonstrated that afterslip persisted for at least three years after the earthquake using GNSS observations. GNSS stations installed on the southeastern side of the Hinagu fault showed a southward displacement of approximately 15 cm over about three years, with 11 cm of this displacement occurring within eight months after the earthquake. Nakao et al. (2019) also indicated an exponential decay of displacement using numerous GNSS stations. Toda et al. (2021) suggested that the in situ-measured surface afterslip represents the surface manifestation of afterslip. Although the absolute slip rates differ, the decaying trend of the displacement observed in our study (Figure 4) qualitatively agrees with the behavior reported by these geodetic studies. The results of this study, indicating that surface afterslip persisted for 6–7 years after the earthquake with a gradual decay, are consistent with the overall spatiotemporal changes identified in previous geodetic findings.

Based on our results and other geodetic observations, surface afterslip following the Kumamoto earthquake occurred in the northern part of the Hinagu fault, near its junction with the Futagawa fault. In this section of the fault, surface ruptures occurred not only during the mainshock but also during the foreshock (Sugito et al., 2016; Kumahara et al., 2022). The repeated surface faulting associated with both a foreshock and a mainshock is rare worldwide (Sugito et al., 2016), and the subsequent occurrence of surface afterslip in the same section is exceptional. This is possibly related to the fact that this segment is located at the junction of the Hinagu and Futagawa faults.

Surface afterslip, similar to that observed after the Kumamoto earthquake, has been reported for past intraplate earthquakes. Regarding the amount and duration of surface afterslip, displacements of up to ~20 cm occurred within several months following the 2014 South Napa earthquake (M 6.0) on the West Napa fault zone and the 2022 Guanshan–Chihshang earthquake (M_w 6.8) on the Yuli fault (Lienkaemper et al., 2016; Wang et al., 2024). Furthermore, surface afterslip persisted for six years with maximum displacements of ~30 cm following the 1944 Bolu–Gerede earthquake (M_w 7.3) on the North Anatolian fault and the 2004 Parkfield earthquake on the San Andreas fault (Lienkaemper and McFarland, 2017; Cakir et al., 2005). For the Kumamoto earthquake we studied, surface afterslip of ~40 cm occurred over a six-year period. Compared with previous cases, the duration is relatively long, while the displacement is consistent with previous cases.

As shown by this and previous studies, surface afterslip lasting several years can occur along intraplate active faults following an earthquake. From the perspective of post-earthquake recovery, even if damaged surface structures and subsurface infrastructures are repaired immediately after an earthquake, they may be re-damaged by subsequent surface afterslip (Toda et al., 2021). Therefore, particularly for critical subsurface infrastructures such as water and gas pipelines—whose repair would require considerable time and cost—it is essential to consider surface afterslip, especially where subsurface infrastructures cross faults. This includes incorporating flexibility to accommodate displacements on the order of tens of centimeters, or postponing full-scale restoration until displacement has been confirmed to have ceased.

Acknowledgements

We are grateful to Mr. Fumitaka Sakamoto for valuable support during the field surveys. This study was supported by JSPS KAKENHI Grant Numbers JP18H03601, JP20J22288, JP23K18735, and the Fukada Grant-in-Aid for Geology Field Research from the Fukada Geological Institute. We used ChatGPT (OpenAI) and Grammarly to improve the English grammar and readability of the manuscript. The authors carefully reviewed and edited the content to ensure the accuracy of the scientific descriptions. Finally, we would like to thank Dr. Shinji Toda and an anonymous reviewer for their insightful comments and constructive suggestions, which greatly improved the quality of this manuscript.

Data and code availability

No custom code was used in this study. Field data were plotted using Microsoft Excel (Microsoft Corp.), and maps were created using QGIS (version 3.28.13). The source field data on the locations and displacements of the surface afterslip are available at https://doi.org/10.5281/zenodo.17732652. 5-m-mesh digital elevation models are available on the Fundamental Geospatial Data issued by the Geospatial Information Authority of Japan website (https://www.gsi.go.jp/kiban/). 30-m-mesh digital surface models are available on the Japan Aerospace Exploration Agency website (https://www.eorc.jaxa.jp/ALOS/jp/dataset/aw3d30/aw3d30_j.htm). Earthquake distribution data are available on the JMA website (https://www.data.jma.go.jp/eqev/data/daily_map/index.html).

Competing interests

The authors declare that they have no competing interests.

References

Baize, S. and Scotti, O. Main lessons about the M=6 Napa (California) earthquake and its effects. In *9ème Colloque National AFPS*. 2015.

Cakir, Z., Akoglu, A., Belabbes, S., Ergintav, S., and Meghraoui, M. Creeping along the Ismetpasa section of the North Anatolian fault (Western Turkey): Rate and extent from InSAR. *Earth and Planetary Science Letters*, 238(1–2):225–234, Sept. 2005. doi: 10.1016/j.epsl.2005.06.044.

Churchill, R. M., Werner, M. J., Biggs, J., and Fagereng, A. Afterslip Moment Scaling and Variability From a Global Compilation of Estimates. *Journal of Geophysical Research: Solid Earth*, 127(4), Apr. 2022. doi: 10.1029/2021jb023897.

Dhar, S., Muto, J., Ohta, Y., and Iinuma, T. Heterogeneous rheology of Japan subduction zone revealed by postseismic deformation of the 2011 Tohoku-oki earthquake. *Progress in Earth and Planetary Science*, 10(1), Feb. 2023. doi: 10.1186/s40645-023-00539-1.

Fujiwara, S., Yarai, H., Kobayashi, T., Morishita, Y., Nakano, T., Miyahara, B., Nakai, H., Miura, Y., Ueshiba, H., Kakiage, Y., and Une, H. Small-displacement linear surface ruptures of the 2016 Kumamoto earthquake sequence detected by ALOS-2 SAR interferometry. *Earth, Planets and Space*, 68(1), Sept. 2016. doi: 10.1186/s40623-016-0534-x.

Hashimoto, M. Postseismic deformation following the 2016 Kumamoto earthquake detected by ALOS-2/PALSAR-2. *Earth, Planets and Space*, 72(1), Oct. 2020. doi: 10.1186/s40623-020-01285-0.

Himematsu, Y. and Furuya, M. Coseismic and Postseismic Crustal Deformation Associated With the 2016 Kumamoto Earthquake Sequence Revealed by PALSAR-2 Pixel Tracking and InSAR. *Earth and Space Science*, 7(10), Sept. 2020. doi: 10.1029/2020ea001200.

Hong, S. and Liu, M. Postseismic Deformation and Afterslip Evolution of the 2015 Gorkha Earthquake Constrained by InSAR and GPS Observations. *Journal of Geophysical Research: Solid Earth*, 126(7), June 2021. doi: 10.1029/2020jb020230.

Kumahara, Y., Kaneda, H., and Tsutsumi, H. *Surface Ruptures Associated with the 2016 Kumamoto Earthquake Sequence in Southwest Japan*. Springer Nature Singapore, 2022. doi: 10.1007/978-981-19-1150-7.

Lienkaemper, J. J. and McFarland, F. S. Long-Term Afterslip of the 2004M 6.0 Parkfield, California, Earthquake—Implications for Forecasting Amount and Duration of Afterslip on Other Major

Creeping Faults. *Bulletin of the Seismological Society of America*, 107(3):1082–1093, Apr. 2017. doi: 10.1785/0120160321.

Lienkaemper, J. J., DeLong, S. B., Domrose, C. J., and Rosa, C. M. Afterslip Behavior following the 2014 M 6.0 South Napa Earthquake with Implications for Afterslip Forecasting on Other Seismogenic Faults. *Seismological Research Letters*, 87(3):609–619, Mar. 2016. doi: 10.1785/0220150262.

Liu, Y., Cui, X., Hu, Y., Zhang, J., and Chen, Y. Integrated Investigation on Heterogeneous Lower Crust Rheology in Kyushu and Afterslip Behavior Following the 2016 Mw7.1 Kumamoto Earthquake. *Geophysical Research Letters*, 51(7), Apr. 2024. doi: 10.1029/2023gl107606.

Milliner, C., Bürgmann, R., Inbal, A., Wang, T., and Liang, C. Resolving the Kinematics and Moment Release of Early Afterslip Within the First Hours Following the 2016 Mw 7.1 Kumamoto Earthquake: Implications for the Shallow Slip Deficit and Frictional Behavior of Aseismic Creep. *Journal of Geophysical Research: Solid Earth*, 125(9), Sept. 2020. doi: 10.1029/2019jb018928.

Nakao, S., Yakiwara, H., Sakakibara, N., Ito, T., Matsuhiro, K., Nishimura, T., Yamazaki, K., Komatsu, S., Tabei, T., Okubo, M., and Yamashina, T. *3.2 Survey and observation for elucidating the three-dimensional morphology of fault zones and the crustal structure surrounding them*. Ministry of Education, Culture, Sports, Science and Technology and Kyushu University, 2019.

Nakata, T. and Imaizumi, T. *Digital active fault map of Japan*. University of Tokyo Press, 2002.

Noda, A., Takahama, T., Kawasato, T., and Matsu'ura, M. Interpretation of Offshore Crustal Movements Following the 2011 Tohoku-Oki Earthquake by the Combined Effect of Afterslip and Viscoelastic Stress Relaxation. *Pure and Applied Geophysics*, 175 (2):559–572, Oct. 2017. doi: 10.1007/s00024-017-1682-z.

Nurminen, F., Baize, S., Boncio, P., Blumetti, A. M., Cinti, F. R., Civico, R., and Guerrieri, L. SURE 2.0 – New release of the worldwide database of surface ruptures for fault displacement hazard analyses. *Scientific Data*, 9(1), Nov. 2022. doi: 10.1038/s41597-022-01835-z.

Ozawa, S., Nishimura, T., Munekane, H., Suito, H., Kobayashi, T., Tobita, M., and Imakiire, T. Preceding, coseismic, and postseismic slips of the 2011 Tohoku earthquake, Japan. *Journal of Geophysical Research: Solid Earth*, 117(B7), July 2012. doi: 10.1029/2011jb009120.

Pollitz, F. F., Kobayashi, T., Yarai, H., Shibazaki, B., and Matsumoto, T. Viscoelastic lower crust and mantle relaxation following the 14–16 April 2016 Kumamoto, Japan, earthquake sequence. *Geophysical Research Letters*, 44(17):8795–8803, Sept. 2017. doi: 10.1002/2017gl074783.

Scholz, C. H., Wyss, M., and Smith, S. W. Seismic and aseismic slip on the San Andreas Fault. *Journal of Geophysical Research*, 74 (8):2049–2069, Apr. 1969. doi: 10.1029/jb074i008p02049.

Shirahama, Y., Yoshimi, M., Awata, Y., Maruyama, T., Azuma, T., Miyashita, Y., Mori, H., Imanishi, K., Takeda, N., Ochi, T., Otsubo, M., Asahina, D., and Miyakawa, A. Characteristics of the surface ruptures associated with the 2016 Kumamoto earthquake sequence, central Kyushu, Japan. *Earth, Planets and Space*, 68 (1), Nov. 2016. doi: 10.1186/s40623-016-0559-1.

Shu, C., Meng, Z., Wu, Q., Xiong, W., He, L., Zhang, X., and Xu, D. Coseismic and Early Postseismic Deformation Mechanism Following the 2021 Mw 7.4 Maduo Earthquake: Insights from Satellite Radar Interferometry and GPS. *Remote Sensing*, 16(8):1399, Apr. 2024. doi: 10.3390/rs16081399.

Sugito, N., Goto, H., Kumahara, Y., Tsutsumi, H., Nakata, T., Kagohara, K., Matsuta, N., and Yoshida, H. Surface fault ruptures associated with the 14 April foreshock (Mj 6.5) of the 2016 Kumamoto earthquake sequence, southwest Japan. *Earth, Planets and Space*, 68(1), Nov. 2016. doi: 10.1186/s40623-016-0547-5.

Suito, H. Postseismic deformation model of the 2024 Noto Peninsula earthquake, central Japan. *Earth, Planets and Space*, 77(1), July 2025. doi: 10.1186/s40623-025-02228-3.

Toda, S., Kaneda, H., Okada, S., Ishimura, D., and Mildon, Z. K. Slip-partitioned surface ruptures for the Mw 7.0 16 April 2016 Kumamoto, Japan, earthquake. *Earth, Planets and Space*, 68(1), Nov. 2016. doi: 10.1186/s40623-016-0560-8.

Toda, S., Torii, M., Omata, M., Sango, D., and Ishizawa, T. Surface afterslip on the northernmost Hinagu fault associated with the 2016 Kumamoto earthquake. *Active fault Research*, 54:39–56, 2021. doi: 10.11462/afr.2021.54_39.

Wang, Y., Wu, S.-H., Chou, H. L. B., Li, Y.-Y., Cheng, W. S., Ho, A., Chen, J.-M., Liu, S.-C., Hsieh, C.-Y., Duan, S., Min, S. M., Myo, E. M. N., Tsai, Y.-L., Liang, N.-W., Liao, J.-H., Lam, T. Y. A., Chang, E.-W., and Shyu, J. B. H. Surface ruptures of the 2022 Guanshan-Chihshang earthquakes in central Longitudinal Valley area, eastern Taiwan. *Terrestrial, Atmospheric and Oceanic Sciences*, 35(1), Sept. 2024. doi: 10.1007/s44195-024-00077-3.

Wesnousky, S. G. Displacement and Geometrical Characteristics of Earthquake Surface Ruptures: Issues and Implications for Seismic-Hazard Analysis and the Process of Earthquake Rupture. *Bulletin of the Seismological Society of America*, 98(4): 1609–1632, Aug. 2008. doi: 10.1785/0120070111.